*Annals of Botany* **122**: 593–604, 2018
doi: 10.1093/aob/mcy091, available online at www.academic.oup.com/aob

ANNALS OF BOTANY
Founded 1887

# Comparison of population genetic structures of the plant *Silene stellata* and its obligate pollinating seed predator moth *Hadena ectypa*

**Juannan Zhou[1,*], Michele R. Dudash[2], Elizabeth A. Zimmer[3] and Charles B. Fenster[4]**

*[1]Simons Center for Quantitative Biology, Cold Spring Harbor Laboratory, Cold Spring Harbor, NY 11724, USA, [2]Department of Natural Resource Management, South Dakota State University, Brookings, SD 57007, USA, [3]Department of Botany, National Museum of Natural History, MRC 166, Smithsonian Institution, Washington, DC 20013–7012, USA and [4]Department of Biology and Microbiology, South Dakota State University, Brookings, SD 57007, USA*
**For correspondence. E-mail: jzhou@cshl.edu*

Received: 5 November 2017 Returned for revision: 19 March 2018 Editorial decision: 1 May 2018 Accepted: 3 May 2018
Published electronically 30 May 2018

• **Background and Aims** Population genetic structures and patterns of gene flow of interacting species provide important insights into the spatial scale of their interactions and the potential for local co-adaptation. We analysed the genetic structures of the plant *Silene stellata* and the nocturnal moth *Hadena ectypa*. *Hadena ectypa* acts as one of the important pollinators of *S. stellata* as well as being an obligate seed parasite on the plant. Although *H. ectypa* provides a substantial pollination service to *S. stellata*, this system is largely considered parasitic due to the severe seed predation by the *Hadena* larvae. Previous research on this system has found variable interaction outcomes across space, indicating the potential for a geographical selection mosaic.
• **Methods** Using 11 microsatellite markers for *S. stellata* and nine markers for *H. ectypa*, we analysed the population genetic structure and the patterns and intensity of gene flow within and among three local populations in the Appalachians.
• **Key Results** We found no spatial genetic structure in the moth populations, while significant differentiation was detected among the local plant populations. Additionally, we observed that gene flow rates among *H. ectypa* populations were more uniform and that the mean gene flow rate in *H. ectypa* was twice as large as that in *S. stellata.*
• **Conclusions** Our results suggest that although the moths move frequently among populations, long-distance pollen carryover only happens occasionally. The difference in gene flow rates between *S. stellata* and *H. ectypa* could prevent strict local co-adaptation. Furthermore, higher gene flow rates in *H. ectypa* could also increase resistance of the local *S. stellata* populations to the parasitic effect of *H. ectypa* and therefore help to stabilize the *Silene–Hadena* interaction dynamics.

**Key words:** *Silene stellata*, *Hadena ectypa*, pollinating seed predator, population genetics, gene flow.

## INTRODUCTION

Species interactions often occur at spatially discrete scales (Tilman and Kareiva, 1997). Thus, spatial heterogeneity of biotic and abiotic factors among communities can result in differential ecological outcomes for these interactions, leading to a 'geographic selection mosaic' (GSM) (Thompson, 2005). Under the GSM framework, three low-scale phenomena, i.e. geographic selection mosaics, coevolutionary hotspots and trait remixing, lead to highly fluid ecological and genetic structures on the regional level, which in turn determine the broader coevolutionary dynamics on the evolutionary time scale including diversification and speciation (Thompson, 2005).

Spatial genetic structures have strong effects on the coevolutionary dynamics of interacting species for the following reasons. First, if the fitness of a particular genotype of one of the interacting species depends on the genotypic distribution of its partner species, genetic differentiation between populations of the second species could result in differential interaction outcomes among populations. This interaction adds another dimension to the geographic selection mosaic and the resulting genotype by genotype by environment interaction introduces variability to local coevolutionary dynamics (Thompson, 2005).

Secondly, metapopulation processes, including local extinction/recolonization and gene flow, strongly modify local interaction dynamics through the disruption of local genotypic distribution and can lead to coevolutionary outcomes substantially different from the dynamics of isolated populations. For example, a certain range of migration rates among populations helps stabilize host–parasite interactions in a metapopulation framework by reducing the extinction rates for the parasite (Brown, 1969; Hassell *et al.*, 1991). Additionally, theoretical results demonstrate that, for a geographic selection mosaic consisting of two communities in which the pairwise interaction is antagonistic for one and mutualistic for the other, gene flow between the two demes could result in a global evolutionarily stable mutualism and high levels of local maladaptation and trait mismatching (Nuismer *et al.*, 1999). Furthermore, the relative levels of gene flow of the two interacting species can also lead to divergent interaction outcomes (Gandon *et al.*, 1996; Gandon and Michalakis, 2002).

Plant vs. animal comparison provides one of the sharpest contrasts between dispersal abilities of interacting species. Due to the sessile nature of plants, we expect to observe stronger population genetic structure in plants, and especially those with biotic pollination and where seed dispersal is limited (Hamrick and Godt, 1996; Rhodes *et al.*, 2014). However, when the animal species is also a specialized pollinator of the plant, spatial genetic processes of the plant may largely be determined by the pattern of pollen flow mediated by behaviours of the pollinator (Brunet and Holmquist, 2009). Pollinator behaviour can affect population genetic structure both within the plant population (e.g. pollinators restricted to nearest-neighbour plants can increase the level of inbreeding) and among plant populations (e.g. through long-distance pollen dispersal). The potential gene flow asynchrony between a plant and its pollinator blurs the spatial scale of local coevolution and may have implications for plant–pollinator coevolution.

Here we examine the interaction between a native North American species pair: *Silene stellata* and *Hadena ectypa*, through a population genetic structure perspective. Nocturnal moths from the genus *Hadena* and plants of the Caryophyllaceae family, especially in the genus *Silene*, commonly form facultative interactions (Brantjes, 1976*a*, *b*; Kephart *et al.*, 2006; Giménez-Benavides *et al.*, 2007; Reynolds *et al.*, 2012; Prieto-Benítez *et al.*, 2016). The *Silene–Hadena* interactions in most species pairs have been considered to be parasitism (Brantjes, 1976*a*, *b*; Pettersson, 1991; Bopp and Gottsberger, 2004; Reynolds *et al.*, 2012). Unlike the pollinators in more specialized interactions such as fig wasps and yucca moths, larvae of various *Hadena* species consume not only one fruit where they hatch, but also many more flowers and developing fruits before pupation, leading to a considerable fitness reduction for the plant (Reynolds *et al.*, 2012). In addition to interactions with multiple species of *Hadena*, *Silene* species also represent specializations to different pollinator functional groups, coincident with their diverse floral display (Kephart *et al.*, 2006). Closely related species often exhibit highly distinct floral designs; for example, three North American species *S. caroliniana*, *S. stellata* and *S. virginica* exhibit specialization to bee, moth and hummingbird pollination, respectively (Reynolds *et al.*, 2009). The parasitic nature of the *Silene–Hadena* interaction and the great floral diversity in *Silene* beg a mechanistic explanation of how this interaction could persist in multiple lineages over evolutionary time and how transitions to and/or from nocturnal pollination had occurred.

Previous research has shown a correlation between *S. stellata* floral traits and reproductive success (Reynolds, 2009; Kula *et al.*, 2013; Zhou, 2017), corroborating the possibility of ongoing selection on floral traits by *H. ectypa* or by mutualist moth pollinators. Therefore, an important question is whether gene flow patterns of the interacting species at this fine spatial scale would promote or hinder coevolution. The goals of this study are to determine the population genetic structure within and among populations of *S. stellata* and *H. ectypa*, in three local populations within their native habitat in North America. Specifically, we quantify genetic diversity, fine-scale spatial genetic structures and migration patterns of these two closely interacting species to provide insight into the ecological structure and context dependency of this interaction on a metapopulation level. This study is one of the first to assess the population genetic structure of a non-pest nocturnal moth. It is also one of the first studies to compare the population genetic structures between plants and their pollinators.

## MATERIALS AND METHODS

### *Study species and their interaction*

*Silene stellata* L. is an infrequent, iteroparous, long-lived perennial herb that is distributed throughout the eastern part of the USA (Fig. 1). The plant flowers from early July through early September at our study sites. It produces white, hermaphroditic, protandrous flowers (average of 25 ovules/pistil; Reynolds *et al.*, 2009), which form panicle inflorescences. A single plant usually produces multiple stems and on average produces approx. 40 flowers in each flowering season (Reynolds *et al.*, 2012). The outcrossing rate is relatively high (approx. 73 %, Reynolds, 2009; >80 %, Zhou, 2017). The flowers are pollinated by *Hadena ectypa* as well as by a number of generalist nocturnal moths that are equally effective at pollen transfer (Reynolds *et al.*, 2009; Kula *et al.*, 2013). The obligate seed predating pollinator *H. ectypa* is distributed from Massachusetts west to Minnesota and Kansas, and south to northern Georgia, concordant with the distribution of *S. stellata* (Schweitzer *et al.*, 2011; Nelson, 2012). Adult male and female *H. ectypa* collect nectar in the flowers of *S. stellata* with pollination taking place simultaneously. Oviposition behaviour follows nectaring, as female moths lay single or multiple eggs at the base of the ovary or on the ovary wall (Zhou *et al.*, 2016*a*). Forty per cent of visits are followed by oviposition (Kula *et al.*, 2013). The newly hatched larva bores into the ovary and develops through the third instar therein before starting to forage between flowers and plants. A larva can consume up to 40 flowers and/or unhardened fruits under laboratory conditions (Reynolds *et al.*, 2012). The larvae pupate underground, and *H. ectypa* exhibits a univoltine life history at our study sites. A multiyear study conducted in the same sites as investigated here documented fruit predation rates of 10–30 % (Reynolds *et al.*, 2012). The same study also found that the contribution of *H. ectypa* to pollination of *S. stellata* was equal to the co-pollinators in one year, while it was significantly lower in the other year. Furthermore, depending on the relative densities of the co-pollinators, the net outcome of this interaction is spatially and temporally variable on a local scale but overall is negative (Reynolds *et al.*, 2012).

In contrast to the predominant diploidy of *Silene* species distributed in the Old World, the vast majority of North American *Silene* have been shown to be polyploids, including tetra-, hexa- and octoploids, with tetraploids being the most common type (Popp and Oxelman, 2007). It is unclear whether the lineage containing *S. stellata* was formed through autopolyploidization or allopolyploidization (Popp and Oxelman, 2007). Either type of polyploidy, in any case, introduces a number of technical complications for the development of microsatellite markers and the downstream genotyping (Zhou *et al.*, 2016*b*; discussed below).

### *Study sites*

We collected plant and animal tissues in the Appalachians from three local sites near Mountain Lake Biological Station in Giles County, VA, USA: Meadow (37.348296°, –80.544301°,

elevation approx. 1100–1300 m), Windrock (37.413889°, –80.519444°, elevation approx. 1300 m) and Woodland (37.355415°, –80.553469°, elevation approx. 1100–1300 m) (Fig. 1). The Meadow and Woodland sites are about 1.5 km apart, and both are isolated from the Windrock site by 7–8 km.

Among these three local populations, Meadow has the largest population size of *S. stellata*, consisting of many thousands of plants, while the Woodland site has a lower plant density and consists of several hundred individuals. Windrock is the smallest population, with only about 100 plants. These three sites also represent a wide range of habitats of *S. stellata*. The Meadow population is located on a powerline cut that is approx. 1 km long and 40 m wide and devoid of woody canopy. Woodland is a former chestnut forest and currently consists of mainly mature oak and hickory trees. Windrock is an exposed west-facing site with wind-topped oak trees near the Appalachian trail.

We focus our study on this relatively small region with only three local populations for three main reasons: first, a previous study with the European *Silene latifolia* and *Hadena bicruis* demonstrated a discordant population genetic structure for the two interacting species over a spatial scale of 1000 km (Magalhaes *et al.*, 2011) and we wished to investigate whether this pattern was evident at much smaller spatial scales. Secondly, in >20 years of surveys, we have not found any other populations of *S. stellata* defined by the triangle formed by the three sites, or near any of the three sites. Thirdly, we have accumulated ecological data including local selection and population dynamics in these three local populations in the past 20 years. Our study of the spatial genetic structure of these populations can be integrated naturally with these existing data to provide a comprehensive picture about the interaction dynamics on the local level. Additionally, the European species *S. latifolia* showed significant genetic differentiations between sub-populations separated by only a few hundred metres (Barluenga *et al.*, 2010). Thus, it is reasonable to assume that significant genetic structure of *S. stellata* exists on this spatial scale, but whether that of *H. ectypa* does as well is one of the focal questions of this investigation.

### *Silene tissue collection*

In the summer of 2011, we collected leaf tissue from 111 *S. stellata* plants. In the Meadow population, which had the highest plant density, a total of 40 plants were sampled along three transects with approx. 13 plants collected along each transect. Thirty-two and 39 plants were collected along two transects in Windrock and Woodland, respectively, which have much smaller plant populations. Transects were linear and 50–300 m long. We sampled plants that were at least 5 m from each other to refrain from sampling the same plant as some plants produce multiple stems that can be up to 1 m across, and also to sample the greatest genetic diversity within a population. From each plant, a single leaf was removed and stored in silica desiccant (Fisher Scientific). We recorded the GPS co-ordinates of the sampled plants. Genomic DNAs were extracted from 111 *S. stellata* individuals with an AutoGenprep 965/960 machine (AutoGen, Holliston, MA, USA) using the Plant DNA Extraction Kit AGP965/960 following the manufacturer's protocol.

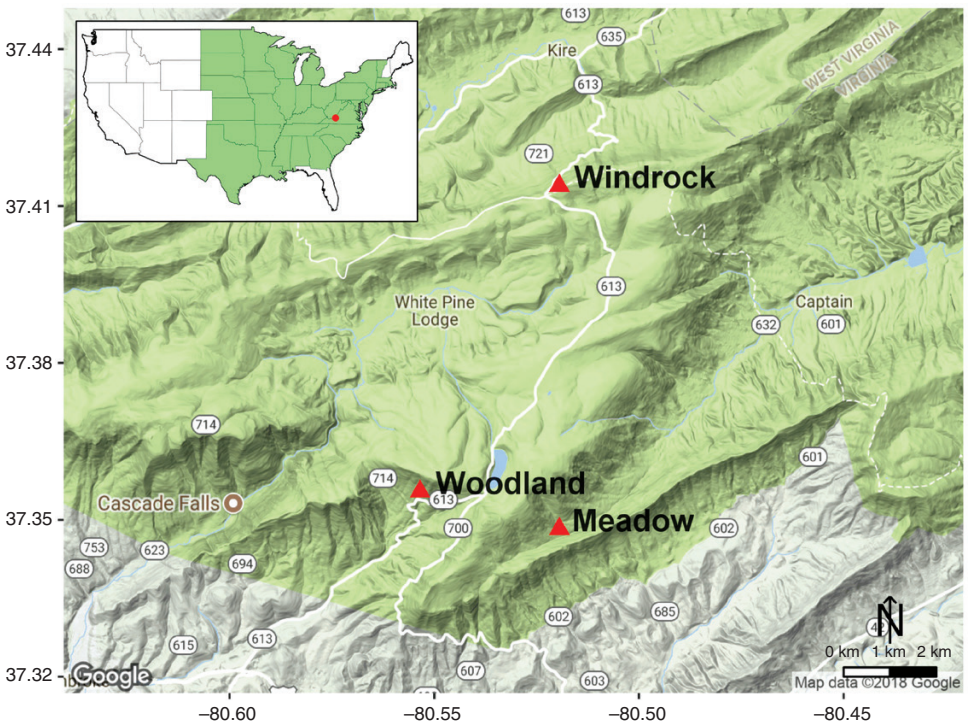


FIG. 1. Geographical locations of three *Silene stellata* and *Hadena ectypa* study populations. GPS co-ordinates: Meadow, 37.348296°, –80.544301°; Windrock, 37.413889°, –80.519444°; Woodland, 37.355415°, –80.553469°. The top left corner shows the general location (in red) of the study area in the USA. Green indicates the distribution of *S. stellata* by states according to the USDA PLANTS database.

*Hadena collection and rearing*

We sampled *H. ectypa* eggs in 2012 from the three sites by collecting *S. stellata* flowers along the same transects described above. To avoid sampling close relatives and to ensure a robust sampling of within-population genetic variation, we collected single flowers from plants that were spaced at least 10 m apart. Flowers were examined under a dissecting microscope for the presence of *H. ectypa* eggs. Eggs were reared in separate Petri dishes and supplied with fresh *S. stellata* fruits until the end of the third instar (about 1 week). The caterpillars were collected in 100 % ethanol and kept in the refrigerator at 4 °C. The tissue samples were stored in this condition for up to 1 year until DNA extraction. We kept no record of the exact locations where the larvae were collected, only from what site they were collected. To extract DNA, approx. 1 g of larval tissue was placed in a 1.5 mL centrifuge tube that was first frozen in liquid nitrogen. The tissue was then ground with a Micro Pestle and then DNA was extracted from the macerated tissue according to the Qiagen Blood & Tissue kit (QIAGEN, Valencia, CA, USA), following the manufacturer's protocol. We extracted DNA from a total of 96 *H. ectypa* larvae (sample size for each population: Meadow $n = 32$, Windrock $n = 31$, Woodland $n = 33$).

*Isolation of microsatellite markers and genotyping*

We collected genotypic data for 11 novel microsatellite loci designed for *S. stellata* with di- or trinucleotide repeats (Zhou *et al.*, 2016*b*). Genotypes of *H. ectypa* samples were obtained for a total of nine microsatellite loci. Eight loci previously designed for *H. bicuris* (Magalhaes *et al.*, 2011) were tested in eight *H. ectypa* individuals. Of the eight tested, five loci (namely Hb02, Hb12, Hb19, Hb24 and Hb29) produced bands consistently and were polymorphic. Additionally, we tested 72 candidate microsatellite loci designed with the program MSATCOMMANDER (Faircloth, 2008) after next-generation sequencing of one *H. ectypa* genomic DNA sample, and successfully identified and characterized four additional polymorphic loci (namely He58, He59, He62 and He66; Supplementary Data Table S1).

DNA amplification was performed with fluorescently labelled forward primers (FAM- or HEX-) in 10 μL reactions, using the QIAGEN Type-it® Microsatellite PCR Kit. Each reaction contained the following components: approx. 10 ng of genomic DNA, 5 μL of the 2× Multiplex PCR Master Mix, 1 μL of the forward primer and 1 μL of the reverse primer (final concentration of the primers: 0.2 μM). A touchdown PCR protocol was performed in a BIO-RAD T100 thermocycler (Bio-Rad, Hemel Hempstead, UK) using the following conditions: 95 °C for 5 min; five cycles at 95 °C for 30 s, 60 °C for 1.5 min and 72 °C for 30 s; 28 cycles at 95 °C for 30 s, 55 °C for 1.5 min and 72 °C for 30 s; and a final extension at 60 °C for 30 min. PCR products were diluted in nuclease-free water (dilutions ranged from 1:10 to 1:50), and 1 μL of each dilution was added to 9 μL of HiDi formamide with 1 μL of ROX standard (DeWoody *et al.*, 2004). Samples were heated to 95 °C for 6 min, cooled to 4 °C for 6 min and loaded onto an ABI 3730×l automated capillary sequencer with a 50 cm, 96 channel array containing POP-7 polymer for fragment analysis at the Laboratories of Analytical Biology (LAB) of the Smithsonian National Museum of Natural History. Fragment patterns were then visualized and scored using the GeneMapper V3.7 software (Applied Biosystems, Foster City, CA, USA). PCR and fragment profiling conditions were identical for *S. stellata* and *H. ectypa.*

*Genetic diversity within populations*

Levels of genetic diversity in the *S. stellata* and *H. ectypa* populations were evaluated by calculating the following statistics using the software Genodive version 2.0b27 (Meirmans and Van Tienderen, 2004): the number of alleles per locus ($A$), effective number of alleles ($A'$, number of alleles in a population weighted for their frequencies), observed heterozygosity ($H_o$) and expected heterozygosity ($H_e$).

Due to the tetraploidy of *S. stellata*, allelic dosage cannot be determined for partial heterozygotes (e.g. an individual showing two alleles A, B on a given locus can have AAAB, AABB or ABBB as the underlying genotype). Genodive allows the unbiased estimations of allele frequencies and $H_e$ within populations for data containing partial heterozygotes in a maximum likelihood framework under the assumption of random mating (De Silva *et al.*, 2005). We used Genodive to characterize genetic diversity and pairwise differentiation between populations for both the tetraploid *S. stellata* and the diploid *H. ectypa*, to ensure consistency across the analyses.

We also calculated $G_{IS}$ (Nei, 1987) in each population for each locus as well as across all loci to evaluate the degree of inbreeding. $G_{IS}$ relates the observed heterozygosity within subpopulations to the expected heterozygosity, ranging from –1 to 1. A positive $G_{IS}$ value indicates an excess of homozygotes and thus the presence of inbreeding. In addition, each population was tested for departure from Hardy–Weinberg equilibrium (HWE) within each locus and across all loci. For the tetraploid *S. stellata*, $H_o$ was calculated as gametic heterozygosity, i.e. 1.0 minus the probability that two random alleles drawn from the individual are the same: AAAA = 0, AAAB = 0.50, AABB = 0.66, AABC = 0.83 and ABCD = 1 (Bever and Felber, 1992; Moody *et al.*, 1993).

*Population structure analysis and differentiation*

We used the Bayesian model-based program STRUCTURE 2.3.4 (Pritchard *et al.*, 2000) to test for the optimal number of genetic groups (denoted $K$ hereafter) and estimated admixture proportions for each individual. To determine the optimal number of genetic clusters, we performed 20 independent runs for each $K = 1$–8 (Evanno *et al.*, 2005), applying the admixture model in 20 replicates using a burn-in period of 10 000 followed by 10 000 steps. For better detection of subtle population structure given the relatively small spatial scale, we chose correlated allele frequencies among proposed clusters following the suggestion by Falush *et al.* (2003), and allowed the degree of admixture ALPHA to be inferred from the data. Given the adjacency of the study populations, we used sampling location as prior information by setting LOCPRIOR = 1. The use of prior information has been suggested to be better at detecting

weak divergence, while at the same time being unbiased toward spurious structures (Hubisz *et al.*, 2009; Pritchard *et al.*, 2010). The true $K$ was determined using both estimates of the posterior probability of the data for a given $K$ (Pritchard *et al.*, 2000) and $\Delta K$ (Evanno *et al.*, 2005). Admixture plots corresponding to the best $K$ for each species were generated using Structure Plot V2.0 (Ramasamy *et al.*, 2014). We corroborated the STRUCTURE results by performing $K$-means clustering of individuals based on the analysis of molecular variance (AMOVA) using Genodive (Meirmans and Van Tienderen, 2004; Meirmans, 2012). We used the Bayesian inference criterion (BIC) and pseudo-$F$ statistic (Caliński and Harabasz, 1974) to select the best number of clusters ($K$ = 1–8). The pseudo-$F$ statistic has better statistical properties than BIC but is not defined for $K = 1$ (Meirmans, 2012). BIC is defined for any $K > 0$, and therefore is useful for detecting whether there is any underlying genetic structure.

We chose Hedrick's $G'_{ST}$ (Hedrick 2005) as the measure of genetic differentiation between and among populations. $F_{ST}$ and its analogue $G_{ST}$ are influenced by the degree of within-population polymorphism. Specifically, when large numbers of alleles are maintained within individual populations, both $H_S$ and $H_T$ can approach 1, even when different alleles are maintained in different populations, causing downwardly biased estimates of genetic differentiation (Hedrick, 1999, 2005). Hedrick's $G'_{ST}$ addresses this challenge by scaling the observed value of differentiation by the maximum possible value given the level of polymorphism, and therefore allows the comparison of levels of genetic differentiation between *S. stellata* and *H. ectypa*, given the difference in allelic richness between these two species. We estimated single-locus and multilocus $G'_{ST}$ values and their significance with 9999 permutations in Genodive. A maximum likelihood method was utilized to correct for unknown dosage of the alleles for *S. stellata* (Meirmans, 2013).

### *Gene flow patterns between populations*

We used the coalescent-based program MIGRATE-N 3.6.11 (Beerli and Palczewski, 2010) to test hypotheses about migration patterns and to estimate gene flow rates between populations. Five migration models were evaluated. All models contain three parameters of population sizes and differ in patterns of migration: (1) a full model with six directional migration rates; (2) a model with three symmetrical migration rates; (3) a model with two directional migration rates between Meadow and Woodland; (4) a model with one undirected migration rate between Meadow and Woodland (Windrock is considered an isolated population under models 3 and 4, given its relative isolation from Meadow and Woodland); and (5) a null model consisting of only population sizes and no migration. We estimated the mutation-scaled effective sizes $\Theta = 4N_e\mu$ (or $\Theta = 8N_e\mu$ for the tetraploid *S. stellata*; Beerli, 2012), where $N_e$ is the effective population size and $\mu$ is the mutation rate, as well as mutation-scaled migration rates $M = m/\mu$, where $m$ is the immigration rate per generation. We used Bayes factors for model comparison based on marginal likelihood values approximated with thermodynamic integration (Beerli, 2012).

We used the Brownian motion mutation model with mutation rate estimated from the data for each locus (see the Results). For each locus, we performed parallel runs of 50 replicates, each consisting of a burn-in period of 100 000 Markov chain Monte Carlo (MCMC) steps, followed by 1 000 000 steps. Samples were recorded every 50 steps, resulting in a total of 20 000 recorded parameter values for each replicate. We used a heating scheme with four changes with temperatures 1.00, 1.50, 3.00 and 1 000 000.00, in order to improve the estimation of marginal likelihood (Beerli, 2009). A random genealogy and parameter values inferred by an $F_{ST}$ -based method were used as the initial condition for each chain. Prior distributions for $\Theta$ and $M$ were uniformly distributed with boundaries 0–200 and 0–5000, respectively.

Because MIGRATE-N only accepts diploid genotypes, we prepared pseudo-diploid data for *S. stellata.* In particular, we inferred the underlying genotypes for partial heterozygotes using the maximum likelihood procedure in Genodive (e.g. an individual with alleles A, B and C on a locus was inferred as AABC, ABBC or ABCC, depending on which configuration had the highest likelihood) (Meirmans, 2013). We then converted the inferred tetraploid genotypes to pseudo-diploid genotypes by placing the four alleles of an individual on a locus on two separate data lines, following the instruction by Beerli (2012). Therefore, for each population, we had twice as many pseudo-diploid samples as the number of tetraploid individuals (number of pseudo-diploid samples: Meadow, $n = 80$; Windrock, $n = 64$; Woodland, $n = 78$). This procedure does not change the actual number of alleles sampled, and thus the estimation of the confidence intervals is not affected. Parallel computation of MIGRATE-N was conducted using computational resources at the Maryland Advanced Research Computing Center (MARCC).

## RESULTS

### *Neutral genetic variation within populations*

*Silene stellata.* We genotyped 111 individuals at 11 microsatellite loci. All loci were highly polymorphic, with 342 alleles found over all loci (average number of alleles per locus = 31.1). The number of alleles per locus ranged from 16 (loci 3R and S12) to 55 (S44) (Supplementary Data Table S2). The population with the highest average number of alleles was Meadow (22.6), followed by Woodland (21.3) then by Windrock (18.5). We also observed a prevalence of private alleles (alleles present in samples from only one population) in all loci and in all populations. The largest number of private alleles observed was ten (locus S44 in Windrock). Additionally, large numbers of rare alleles were found to be common: over all loci, 141 alleles (41.2 %) were present at a frequency <2 % among all populations.

High single-locus $H_e$ was observed in all three populations, ranging between 0.599 (S12 in Meadow) and 0.953 (S71 in Meadow) (Supplementary Data Table S2). Over all loci, Windrock had the highest $H_e = 0.879$, followed by Woodland ($H_e = 0.870$) and Meadow ($H_e = 0.864$) (Table 1). Although we observed significant $G_{IS}$ scores in some population by locus combinations (Supplementary Data Table S2), multilocus $G_{IS}$ values in all three populations were positive, but not significant (Table 1). Note that due to the technical difficulty caused by

TABLE 1. *Genetic diversity of* Silene stellata *and* Hadena ectypa *in three local populations and across populations near Mountain Lake Biological Station*

| Population | *S. stellata* | | | | | | *H. ectypa* | | | | | |
|---|---|---|---|---|---|---|---|---|---|---|---|---|
| | *n* | *A* | *A'* | $H_o$ | $H_e$ | $G_{IS}$ | *n* | *A* | *A'* | $H_o$ | $H_e$ | $G_{IS}$ |
| Meadow | 40 | 22.636 | 9.196 | 0.765 | 0.864 | 0.115n.s. | 32 | 6.333 | 2.793 | 0.358 | 0.554 | 0.354*** |
| Windrock | 32 | 18.455 | 8.768 | 0.698 | 0.879 | 0.206n.s. | 31 | 6 | 2.892 | 0.373 | 0.567 | 0.341*** |
| Woodland | 39 | 21.273 | 8.582 | 0.770 | 0.870 | 0.115n.s. | 33 | 7.222 | 3.080 | 0.326 | 0.582 | 0.440*** |
| Overall | 111 | 31.091 | 8.814 | 0.757 | 0.887 | 0.146n.s. | 96 | 9.333 | 2.884 | 0.352 | 0.569 | 0.379*** |

Results were based on 11 microsatellite loci for *S. stellata* and nine microsatellite loci for *H. ectypa*.

*n* = number of individual sampled; *A* = number of alleles; *A'* = effective number of alleles; $H_o$ = observed heterozygosity; $H_e$ = expected heterozygosity; $G_{IS}$ = inbreeding coefficient.

*** $P < 0.001$; n.s., not significant.

partial heterozygotes, the $H_o$ values were not estimated based on unbiased gametic heterozygosity rates, and assessments of $G_{IS}$ and HWE were therefore biased downward.

*Hadena ectypa.* From the 96 *H. ectypa* individuals genotyped for nine microsatellite loci, 84 alleles were found over all loci and populations. The average number of alleles per locus was much lower than in *S. stellata* (9.3 in *H. ectypa*, compared with 31.1 in *S. stellata*). Across all populations, Hb12 had the lowest number of alleles (3) and He59 had the highest (20) (Supplementary Data Table S1). The population with the highest average number of alleles was Woodland (7.2), followed by Meadow (6.3) and Windrock (6.0). The observed heterozygosity averaged over all loci ranged between 0.326 and 0.373 (Table 1). With few exceptions, we observed a strong heterozygote deficit in all loci and in all three populations. Additionally, most of the population by locus combinations showed significant deviation from HWE (Supplementary Data Table 1). Over all loci, all three populations presented significant deviation from HWE ($P < 0.001$), with inbreeding coefficients ranging from 0.341 (Windrock) to 0.440 (Woodland) (Table 1).

### *Neutral genetic divergence between populations*

*Silene stellata.* We found a significant level of neutral genetic differentiation among the three local populations (global $G'_{ST} = 0.09$, $P < 0.001$). Pairwise $G'_{ST}$ values were significant between Meadow and Windrock ($G'_{ST} = 0.146$, $P < 0.005$), and Woodland and Windrock ($G'_{ST} = 0.215$, $P < 0.005$), but only trended towards being significant between Meadow and Woodland ($G'_{ST} = 0.081$, $P = 0.087$) (Table 2; Supplementary Data Table S3).

The optimal number of genetic clusters using STRUCTURE for the *S. stellata* samples according to the $\Delta K$ criterion is $K = 2$ (Supplementary Data Fig. 1), while the posterior probability criterion supported the existence of six genetic groups (Supplementary Data Fig. 2). For $K = 2$, The similarity between Meadow and Woodland and their divergence from Windrock were revealed by their population admixture proportions: Meadow (0.089, 0.911); Woodland (0.086, 0.914); Windrock (0.666, 0.334) (Fig. 2). The hypothesis of $K = 2$ was further supported by the AMOVA *K*-means clustering based on both BIC and the pseudo-*F* statistic.

TABLE 2. *Pairwise and global* G-*statistics* ($G'_{ST}$; *Hedrick, 2005*) *between three local populations of* Silene stellata *and* Hadena ectypa

| | *Silene stellata* | | | *Hadena ectypa* | | |
|---|---|---|---|---|---|---|
| | Global $G'_{ST} = 0.09$, $P < 0.001$ | | | Global $G'_{ST} = 0.005$, $P > 0.10$ | | |
| | M | R | W | M | R | W |
| M | – | ** | ** | – | n.s. | n.s. |
| R | 0.146 | – | n.s. | –0.002 | – | n.s. |
| W | 0.081 | 0.215 | – | 0.008 | 0.008 | – |

Results were based on 11 microsatellite loci for *S. stellata* and nine microsatellite loci for *H. ectypa*.

M = Meadow; R = Windrock; W = Woodland.

$G'_{ST}$ values in the lower matrix and significance (***$P < 0.001$; **$P < 0.01$; *$P < 0.05$; n.s., not significant) in the upper matrix.

*Hadena ectypa.* Neutral genetic divergence among the three studied populations was very low and not significant. Pairwise $G'_{ST}$ ranged between 0.001 (Meadow vs. Windrock) and 0.005 (Windrock vs. Woodland), with global $G'_{ST} = 0.003$ ($P = 0.270$). The single locus global $G'_{ST}$ ranged from 0.000 to 0.038 (Table 2; Supplementary Data Table S4).

In contrast to the insignificant $G'_{ST}$, both posterior probabilities of the data and $\Delta K$ identified $K = 3$ as the highest probable genetic structure between the three sample populations (Supplementary Data Figs 3 and 4). Furthermore, the two *K*-means clustering statistics supported different number of clusters: $K = 4$ for the BIC and $K = 2$ for the pseudo-*F* statistic.

### *Gene flow between populations*

*Silene stellata.* Bayes factors calculated as the ratio of likelihoods between two competing models strongly supported the full model with directional gene flow between all populations against the four alternative models (Bayes factor $K > 100$ for all comparisons between the full model and alternative models; Kass and Raftery, 1995). Among the three populations, Woodland had the largest effective population size estimate using the Bayesian approach ($\Theta = 8N_e\mu = 3.575$), followed

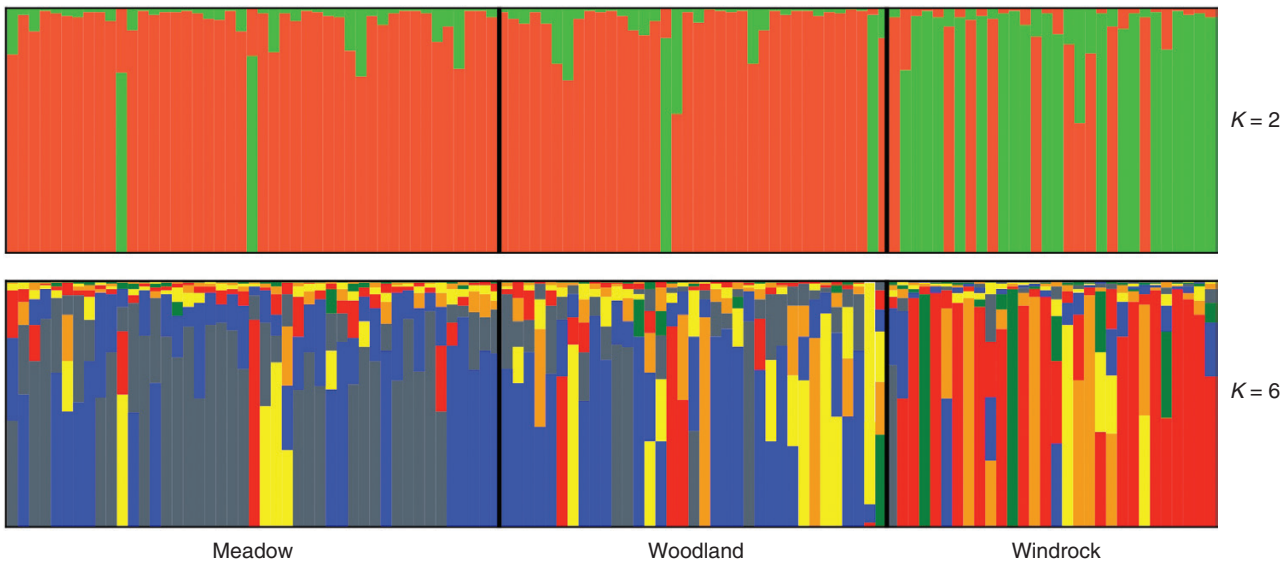


FIG. 2. Estimated population structure of *Silene stellata*, for $K = 2$ and $K = 6$, based on genotypes of 111 *S. stellata* individuals using 11 microsatellite loci. Individuals are represented by vertical bars representing estimated genomic proportions corresponding to the proposed *K*.

TABLE 3. *Mean and 95 % confidence intervals of mutation-scaled population sizes (*$\Theta = 8N_e\mu$ *for* Silene stellata*,* $\Theta = 4N_e\mu$ *for* Hadena ectypa*) and directional migration rates (*$M = m/\mu$*) between three local populations of* S. stellata *and* H. ectypa *based on Bayesian inference of effective sizes and migration rates using MIGRATE-N 3.2.6*

| Parameter | *S. stellata* | | *H. ectypa* | |
|---|---|---|---|---|
| | Mean | 95 % CI | Mean | 95 % CI |
| $\Theta_M$ | 2.55 | 0–5.73 | 1.371 | 0–4.67 |
| $\Theta_R$ | 1.38 | 0–4.67 | 1.209 | 0–4.40 |
| $\Theta_W$ | 3.58 | 0–7.07 | 2.861 | 0–6.27 |
| $M_{R\to M}$ | 14.89 | 16.30–20.13 | 34.336 | 0–120.00 |
| $M_{W\to M}$ | 42.47 | 33.73–49.07 | 40.094 | 0–126.67 |
| $M_{M\to R}$ | 5.76 | 2.67–6.50 | 52.393 | 0–136.67 |
| $M_{W\to R}$ | 15.93 | 13.80–17.73 | 65.220 | 0–146.67 |
| $M_{M\to W}$ | 25.53 | 19.73–31.20 | 47.889 | 0–130.00 |
| $M_{R\to W}$ | 26.89 | 18.40–33.47 | 47.200 | 0–130.00 |

M = Meadow; R = Windrock; W = Woodland.

by Meadow ($\Theta = 2.551$), with Windrock being the smallest ($\Theta = 1.377$) (Table 3; Fig. 3A). Note that the coefficient 8 in $\Theta = 8N_e\mu$ results from the fact that *S. stellata* is a tetraploid. Estimation of migration rates ($M = m/\mu$) between populations using the Bayesian approach were variable and asymmetrical among populations. The highest migration rate was from Woodland to Meadow ($M = 42.470$), which was almost ten times stronger than from Meadow to Windrock ($M = 5.759$) (Table 3; Fig. 3A).

*Hadena ectypa.* Bayes factors also supported the full migration model for *H. ectypa*. Similar to *S. stellata*, the Woodland population was identified as having the largest effective population size ($\Theta = 4N_e\mu = 2.861$), followed by Meadow ($\Theta = 1.371$), with Windrock the smallest ($\Theta = 1.209$) (Table 3; Fig. 3B). Migration rates between populations of *H. ectypa* were more uniform than those of *S. stellata*, with *M* ranging between 34.336 (from Windrock to Meadow) and 65.220 (from Woodland to Windrock) (Table 3; Fig. 3B).

## DISCUSSION

Discordance in the population genetic structures and patterns of gene flow is of potential importance for the coevolution between interacting species in that they do not only provide the spatial background for the interaction, but could also actively determine the coevolutionary outcome (Gandon *et al.*, 1996; Nuismer *et al.*, 1999). The *Silene–Hadena* interactions range from parasitic to potentially mutualistic (Kephart *et al.*, 2006), dependent upon a suite of ecological factors influencing the ecological outcome and potential coevolutionary trajectory of this interaction. The goals of this study are to compare the fine-scale spatial population genetic structures between *S. stellata* and *H. ectypa* in order to understand the potential for local co-adaptation and the stability of this interaction. We found that *S. stellata* exhibits significant genetic differentiation between populations separated by >7 km while *H. ectypa* demonstrates no genetic differentiation between populations.

### *Within-population genetic diversity*

For *S. stellata,* all loci showed very high levels of variability, and rare alleles were also very common. A number of studies utilizing microsatellites in polyploid plants have found similarly high levels of rare alleles and allelic richness (Truong *et al.*, 2007; Donkpegan *et al.*, 2015). Rare alleles in tetraploid genomes have been suggested to be lost at a much slower rate than in diploids, and tetraploids often exhibit higher polymorphism than related diploids (Bever and Felber, 1992). This can be partially understood to be the consequence of the increased


FIG. 3. Patterns of gene flow between three local populations of *Silene stellata* (A) and *Hadena ectypa* (B) near Mountain Biological Station in Giles County, VA, based on MIGRATE-N 3.2.6 using 11 microsatellite markers for *S. stellata* and nine microsatellite markers for *H. ectypa*. Each circle represents a study population, with the corresponding mutation-scaled effective population size ($\Theta = 8N_e\mu$) shown within the circle. Six directional migration rates ($M = m/\mu$) are shown next to the arrows indicating directional migrations. The sizes of the circles and the weights of the arrows are scaled by the corresponding measures of effective population size or migration rate.

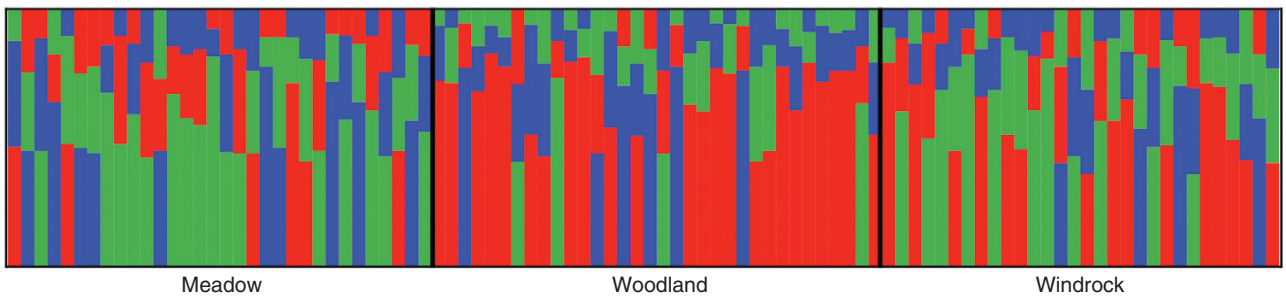


FIG. 4. Estimated population structure of *Hadena ectypa*, for $K = 3$, based on genotypes of 96 *H. ectypa* individuals on nine microsatellite loci. Individuals are represented by vertical bars representing estimated genomic proportions corresponding to three genetic clusters.

effective population size caused by the doubling of individual genomes, which reduces the effect of genetic drift and allows higher neutral polymorphism.

The unknown dosage of alleles for partial heterozygotes in polyploids makes it challenging to calculate allele frequencies and other summary statistics dependent on allele frequency estimation, such as expected heterozygosity and the fixation index. We estimated population-level allele frequencies using the iterative method of Genodive which maximizes the likelihood of the observed allelic phenotypes (Meirmans, 2013). This procedure is a modification of the expectation-maximization method introduced by De Silva *et al.* (2005) and represents one of the current methods allowing the correction of unknown allelic dosage (Dufresne *et al.*, 2014). While certain biases are introduced by the assumption of random mating, the high allelic richness and high proportion of full heterozygotes across loci should make our estimation of $H_e$, as well as other allele frequency-based statistics including $G'_{ST}$ and gene flow rates, relatively robust.

Because of allelic dosage uncertainty, we cannot directly assess gametic heterozygosity for partial heterozygotes (e.g. for a phenotype AB at a given locus, the underlying genotypes ABBB and AABB have gametic heterozygosity of 0.5 and 0.66). Therefore, our estimate of observed heterozygosity and inbreeding for *S. stellata* could only be based on the frequency of full homozygotes. This makes our estimates of $H_o$ and $G_{IS}$, as well as the test of HWE, conservative for *S. stellata*, since the full homozygosity rate in polyploids is less sensitive to inbreeding than in diploids (Bever and Felber, 1992). In light of this technical difficulty inherent to tetraploidy, our estimates of $H_o$ and $G_{IS}$ did not show significant inbreeding within the three populations of *S. stellata.*

A previous fluorescent dye study showed pollen dispersal distance (mean ± s.e.) of *S. stellata* to be 1.2 ± 0.35 m by diurnal pollinators and 2.2 ± 0.43 m by nocturnal pollinators (Reynolds *et al.*, 2009), while elsewhere (Zhou, 2017), using paternity analysis, we demonstrated that most pollen dispersal is <3 m. Furthermore, *H. ectypa* pollinators of *S. stellata* plants

isolated by 30 m from the main Meadow population deposit very little pollen, suggesting that pollen dispersal between populations will be very low (Kula *et al.*, 2014). Additionally, seeds of *S. stellata* primarily disperse passively through gravity. In other plant species, limited pollen and seed dispersal ability have been known to increase inbreeding (Fenster, 1991*a*, *b*; Richards, 2000; Herlihy and Eckert, 2002; Fenster *et al.*, 2003; Whelan *et al.*, 2009). Other than the possibility that significant inbreeding is masked by the biased estimate of HWE, other factors could counterbalance the effect of short pollen and seed dispersal distances. First, although the pollen dispersal distance is short, the probability that an *S. stellata* individual receives pollen from a single source plant is low (0.05–0.12; Reynolds, 2009), possibly reducing the chance of bi-parental inbreeding. Additionally, a relatively high outcrossing rate of approx. 73 % (Reynolds, 2009) and >80 % using genetic marker approaches (Zhou, 2017) in our *S. stellata* populations could counteract the effect of short pollen/seed dispersal distance.

In contrast to *S. stellata*, we found high levels of inbreeding in *H. ectypa*, with significant multilocus $G_{IS}$ values ranging from 0.341 to 0.440, although *H. ectypa* seems to have a high level of gene flow suggested by the observed weak genetic differentiation. Similar levels of significant inbreeding coefficients were quantified in a microsatellite-based study of the European species *S. latifolia* and *H. bicuris* (Magalhaes *et al.*, 2011). These results suggest that there may be common or shared aspects of *Hadena* behaviour responsible for the high observed inbreeding coefficients across species. In the flowering season of *S. stellata*, female *H. ectypa* often lay multiple eggs within the same flower (Zhou *et al.*, 2016*a*). Additionally, the short pollen dispersal distance suggests that female moths could also lay eggs in adjacent flowers and/or plants. The clustered egg-laying behaviour could potentially cause mating between siblings given the limited movement of larvae and if mating occurs immediately after emergence. Subsequent long-distance dispersal by adults, but especially females, could then result in the lack of population genetic differentiation coupled with strong inbreeding. Another scenario that could produce the observed result would be if there were few adults mating and laying eggs within a local population, which could lead to inbreeding, followed by dispersal.

The high molecular genetic diversity found in *S. stellata* populations corresponds to significant genetic variation for floral traits (Zhou, 2017), suggesting ample opportunity for *S. stellata* floral traits to respond to selection mediated by *H. ectypa*. In contrast, the limited amount of molecular genetic variation found in populations of *H. ectypa* may indicate similarly low levels of genetic variation and thus a limited potential to respond to selection imposed by the host, *S. stellata*. This extrapolation should be tempered by the generally low observed correlation of molecular variation with heritable variation (Carr and Fenster, 1994; but see Reed and Frankham, 2001; Gilligan *et al.*, 2005).

### *Population genetic structure*

We found a significant global genetic differentiation, noted by the $G'_{ST}$ values of the three *S. stellata* populations consistent with other studies of outcrossing herbaceous plants (Hamrick and Godt, 1996). Pairwise $G'_{ST}$ values were significant for Windrock vs. Meadow and Windrock vs. Woodland, but not significant between Meadow and Woodland. This is not surprising, as Windrock is the most remote population, separated from the other two populations by approx. 8 km, whereas the distance between Meadow and Woodland is approx. 1.5 km.

Both the $\Delta K$ criterion of STRUCTURE and AMOVA *K*-means clustering support the existence of two genetic groups among the three *S. stellata* populations. Additionally, $K = 6$ was identified as the optimal cluster number by STRUCTURE as having the highest posterior probability, suggesting possible genetic structures within the sampled populations. Under $K = 2$, the similarity between Meadow and Woodland and their divergence from Windrock are made obvious by their population admixture proportions (Fig. 2A).

Both the $G'_{ST}$ and STRUCTURE results indicate a gene flow barrier existing between Windrock and the other two populations. In a study of the European species *S. latifolia*, significant differentiation ranging from 0.05 to 0.2 $G'_{ST}$ was observed between sub-populations separated by only a few hundred metres and up to 2 km (Barluenga *et al.*, 2010). However, we found the $G'_{ST}$ between Meadow and Woodland to be only about one-tenth the magnitude of *S. latifolia* under similar isolation and not significant, although these two populations are separated by about 1.5 km. The insignificant $G'_{ST}$ should not be an issue of statistical power since we sampled twice as many plants per *S. stellata* population as the aforementioned cited study. One possible explanation is that Meadow and Woodland were originally connected but recently separated by human-induced fragmentation. Alternatively, it could imply that genetic differentiation in *S. stellata* occurs on a larger spatial scale than in *S. latifolia.* Differences in life history of these two species could potentially explain this discrepancy. *Silene latifolia* is a short-lived diploid perennial that mainly grows in disturbed habitats where demographical fluctuation and even local extinction could be prevalent (Richards *et al.*, 2003), whereas *S. stellata* is a long-lived perennial (M. R. Dudash and C. B. Fenster, unpubl. data). The potentially larger effective population size resulting from the longevity as well as the polyploidy of *S. stellata* could better buffer the effect of genetic drift and result in less genetic differentiation between populations, even under similar levels of gene flow. Tetraploids have half the decrease in rate of loss of heterozygosity (Bever and Felber, 1992; Falconer and Mackay, 1996), which could also contribute to the difference in genetic differentiation between these two species given recent population sub-division.

In contrast, we observed no genetic differentiation between the three populations of *H. ectypa* based on the $G'_{ST}$ estimations. However, Bayesian clustering using STRUCTURE and *K*-means clustering yielded several possibilities for the number of genetic clusters ($K = 3$ for STRUCTURE; $K = 2$ and 4 for *K*-means clustering using the pseudo-*F* statistic and BIC, respectively). For the STRUCTURE result, although a cluster number $K = 3$ was best supported, the population admixture proportions were very similar across all three populations (Fig. 4), suggesting low genetic differentiation between populations and agreeing with the $G'_{ST}$ estimations. Given that the genetic differentiation between sample populations is insignificant while both clustering methods supported more than one genetic cluster, it seems possible that there are underlying

genetic structures within the sampled populations. This may also contribute to the high observed inbreeding coefficients within the sampled populations.

In any case, we believe the 10- to 100-fold difference in the *G*-statistics suggests that gene flow among *H. ectypa* populations occurs much more frequently than among *S. stellata* populations, and that, although high *H. ectypa* movement was observed among all three populations, the approx. 8 km isolation between Windrock and the other two populations creates a barrier for *S. stellata* pollen dispersal (supported by Kula *et al.*, 2014).

The spatial genetic structure in *S. stellata* indicates that pollen carryover rarely happens over distances >8 km. One hypothesis for this restricted pollen movement is that long-distance flight creates a physical barrier for pollen carryover and that although *H. ectypa* and the co-pollinators frequently move between the three populations, pollen carryover rarely happens over such a long distance. This is consistent with previous studies that have shown the average pollen dispersal distance of *S. stellata* to be <3 m (Reynolds *et al.*, 2009; Zhou, 2017). However, these studies do not distinguish between pollen dispersal by *H. ectypa* and by the co-pollinators which account for at least the same amount of pollination as *H. ectypa* (Reynolds *et al.*, 2012). Hence it is also possible that the observed high genetic differentiation in *S. stellata* is due to the more restricted movement of the co-pollinators.

### *Consequences for geographic selection mosaic*

The gene flow asynchrony between the two species may have important implications for the coevolutionary dynamics of the *Silene–Hadena* interaction. First, the significant genetic structure and the restricted gene flow over long distances of *S. stellata* provide the potential for local adaptation of floral traits involved in the interaction with *H. ectypa*. However, the high gene flow rate and the lack of genetic structure of local *H. ectypa* populations may prevent strict local co-adaptation. Secondly, this discrepancy between migration abilities could also have a stabilizing effect. Theoretical work has shown that when gene flow of the parasite is stronger than that of the host, the parasite populations are selected for adaptation to local host types while the host populations are selected to be resistant to all parasite types, promoting trait polymorphism within local host populations (Gandon *et al.*, 1996). High parasite gene flow brings in non-locally adapted genotypes, which in turn increase local host resistance. The increased host resistance could potentially alleviate the negative parasitic effect and stabilize the interaction dynamics.

While previous work conducted in the same populations indicated the possibility of a geographical selection mosaic (Reynolds *et al.*, 2012), the spatial asynchrony of gene flow between *S. stellata* and its pollinating seed parasite *H. ectypa* implies that the coevolutionary dynamics could be determined by the complex interplay between local processes favouring the escape of *S. stellata* from this interaction and the stabilizing effect of spatial processes on the metapopulation level. Similar gene flow asynchrony in the European *S. latifolia–H. bicuris* system was observed in a study area across central Europe (Magalhaes *et al.*, 2011). The recurrent pattern observed on different spatial scales, together with the distinct life history strategies and ploidy levels of *S. stellata* and *S. latifolia*, suggest that gene flow asynchrony could be a robust mechanism influencing the evolution and maintenance of the *Silene–Hadena* interaction between various lineages from the two genera.

## SUPPLEMENTARY DATA

Supplementary data are available online at https://academic.oup.com/aob and consist of the following. Figure S1: mean $\Delta K$ of 20 independent STRUCTURE runs for *Silene stellata* for each $K$ = 2–7. Figure S2: mean posterior probabilities of 20 independent STRUCTURE runs for *Silene stellata* for each $K$ = 1–8. Figure S3: mean $\Delta K$ of 20 independent STRUCTURE runs for *Hadena ectypa* for each $K$ = 2–7. Figure S4: mean posterior probabilities of 20 independent STRUCTURE runs for *Hadena ectypa* for each $K$ = 1–8. Table S1: genetic diversities of nine polymorphic microsatellites of *Hadena ectypa*. Table S2: genetic diversities of 11 polymorphic microsatellites of *Silene stellata*. Table S3: single-locus and multilocus pairwise and global *G*-statistics and corresponding *P*-values of 11 polymorphic microsatellites between three local populations of *Silene stellata*. Table S4: single-locus and multilocus pairwise and overall *G*-statistics and corresponding *P*-values of nine polymorphic microsatellites between three local populations of *Hadena ectypa*.

## ACKNOWLEDGEMENTS

We thank G. Bernasconi for providing fluorescently labelled *H. bicuris* microsatellite markers and advice at the beginning of this research. We also thank Dudash-Fenster UMD lab mates for input throughout this study, University of Virginia's Mountain Lake Biological Station for summer support for J.Z., NSF Doctoral Dissertation Improvement grant DEB-1501799 awarded to J.Z., and NSF DEB-0108285 awarded to C.R.F. and M.R.D. The Smithsonian Institution provided lab space for the molecular work and troubleshooting guidance.

## LITERATURE CITED

**Barluenga M**, **Austerlitz F**, **Elzinga JA**, **Teixeira S**, **Goudet J**, **Bernasconi G. 2010**. Fine-scale spatial genetic structure and gene dispersal in *Silene latifolia*. *Heredity* **106**: 13–24.

**Beerli P. 2009**. How to use MIGRATE or why are Markov chain Monte Carlo programs difficult to use. In: Bertorelle G, Bruford MW, Hauffe HC, Rizzoli A, Vernesi C, eds. *Population genetics for animal conservation*. Cambridge: Cambridge University Press, 39–77.

**Beerli P. 2012**. *Migrate documentation, Version 3.2*. **1**: 119.

**Beerli P**, **Palczewski M. 2010**. Unified framework to evaluate panmixia and migration direction among multiple sampling locations. *Genetics* **185**: 313–326.

**Bever JD**, **Felber F. 1992**. The theoretical population genetics of autopolyploidy. *Oxford Surveys in Evolutionary Biology* **8**: 185–217.

**Bopp S**, **Gottsberger G. 2004**. Importance of *Silene latifolia* ssp. *alba* and *S. dioica* (Caryophyllaceae) as host plants of the parasitic pollinator *Hadena bicruris* (Lepidoptera, Noctuidae). *Oikos* **105**: 221–228.

**Brantjes NBM. 1976*a***. Riddles around the pollination of *Melandrium album* (Mill.) Garcke (Caryophyllaceae) during the oviposition by *Hadena bicruris* Hufn. (Noctuidae, Lepidoptera). 1. *Proceedings of the Koninklijke Nederlandse Akademie Van Wetenschappen Series C – Biological and Medical Sciences* **79**: 1–12.

**Brantjes NBM. 1976*b***. Riddles around the pollination of *Melandrium album* (Mill.) Garcke (Caryophyllaceae) during the oviposition by *Hadena bicruris* Huyn. (Noctuidae, Lepidoptera). 2. *Proceedings of the Koninklijke Nederlandse Akademie Van Wetenschappen Series C – Biological and Medical Sciences* **79**: 127–141.

**Brown JL. 1969**. The buffer effect and productivity in tit populations. *American Naturalist* **103**: 347–354.

**Brunet J**, **Holmquist KGA. 2009**. The influence of distinct pollinators on female and male reproductive success in the Rocky Mountain columbine. *Molecular Ecology* **18**: 3745–3758.

**Caliński T**, **Harabasz J. 1974**. A dendrite method for cluster analysis. *Communications in Statistics – Theory and Methods* **3**: 1–27.

**Carr DE**, **Fenster CB. 1994**. Levels of genetic-variation and covariation for *Mimulus* (Scrophulariaceae) floral traits. *Heredity* **72**: 606–618.

**De Silva HN**, **Hall AJ**, **Rikkerink E**, **McNeilage MA**, **Fraser LG. 2005**. Estimation of allele frequencies in polyploids under certain patterns of inheritance. *Heredity* **95**: 327–334.

**DeWoody JA**, **Schupp J**, **Kenefic L**, **Busch J**, **Murfitt L**, **Keim P. 2004**. It ROX! *Biotechniques* **37**: 348–352.

**Donkpegan ASL**, **Doucet J-L**, **Dainou K**, **Hardy OJ. 2015**. Microsatellite development and flow cytometry in the African tree genus Afzelia (Fabaceae, Caesalpinioideae) reveal a polyploid complex. *Applications in Plant Sciences* **3**: apps.1400097. doi: 10.3732/apps.1400097.

**Dufresne F**, **Stift M**, **Vergilino R**, **Mable BK. 2014**. Recent progress and challenges in population genetics of polyploid organisms: an overview of current state-of-the-art molecular and statistical tools. *Molecular Ecology* **23**: 40–69.

**Evanno G**, **Regnaut S**, **Goudet J. 2005**. Detecting the number of clusters of individuals using the software STRUCTURE: a simulation study. *Molecular Ecology* **14**: 2611–2620.

**Faircloth BC. 2008**. msatcommander: detection of microsatellite repeat arrays and automated, locus-specific primer design. *Molecular Ecology Resources* **8**: 92–94.

**Falconer DS**, **Mackay TFC. 1996**. *Introduction to quantitative genetics*. Harlow, UK: Longman.

**Falush D**, **Stephens M**, **Pritchard JK. 2003**. Inference of population structure using multilocus genotype data: linked loci and correlated allele frequencies. *Genetics* **164**: 1567–1587.

**Fenster CB. 1991*a***. Gene flow in *Chamaecrista fasciculata* (Leguminosae) I. Gene dispersal. *Evolution* **45**: 398–409.

**Fenster CB. 1991*b***. Gene flow in *Chamaecrista fasciculata* (Leguminosae) II. Gene establishment. *Evolution* **45**: 410–422.

**Fenster CB**, **Vekemans X**, **Hardy OJ. 2003**. Quantifying gene flow from spatial genetic structure data in a metapopulation of *Chamaecrista fasciculata* (Leguminosae). *Evolution* **57**: 995–1007.

**Gandon S**, **Michalakis Y. 2002**. Local adaptation, evolutionary potential and host–parasite coevolution: interactions between migration, mutation, population size and generation time. *Journal of Evolutionary Biology* **15**: 451–462.

**Gandon S**, **Capowiez Y**, **Dubois Y**, **Michalakis Y**, **Olivieri I. 1996**. Local adaptation and gene-for-gene coevolution in a metapopulation model. *Proceedings of the Royal Society B: Biological Sciences* **263**: 1003–1009.

**Gilligan DM**, **Briscoe DA**, **Frankham R. 2005**. Comparative losses of quantitative and molecular genetic variation in finite populations of *Drosophila melanogaster*. *Genetics Research* **85**: 47–55.

**Giménez-Benavides L**, **Dötterl S**, **Jürgens A**, **Escudero A**, **Iriondo JM. 2007**. Generalist diurnal pollination provides greater fitness in a plant with nocturnal pollination syndrome: assessing the effects of a *Silene–Hadena* interaction. *Oikos* **116**: 1461–1472.

**Hamrick JL**, **Godt MJW. 1996**. Effects of life history traits on genetic diversity in plant species. *Philosophical Transactions of the Royal Society B: Biological Sciences* **351**: 1291–1298.

**Hassell MP**, **Comins HN**, **May R. 1991**. Spatial structure and chaos in insect population dynamics. *Nature* **353**: 255–258.

**Hedrick PW. 1999**. Perspective: highly variable loci and their interpretation in evolution and conservation. *Evolution* **53**: 313–318.

**Hedrick PW. 2005**. A standardized genetic differentiation measure. *Evolution* **59**: 1633–1638.

**Herlihy CR**, **Eckert CG. 2002**. Genetic cost of reproductive assurance in a self-fertilizing plant. *Nature* **416**: 320–323.

**Hubisz MJ**, **Falush D**, **Stephens M**, **Pritchard JK. 2009**. Inferring weak population structure with the assistance of sample group information. *Molecular Ecology Resources* **9**: 1322–1332.

**Kass RE**, **Raftery AE. 1995**. Bayes factors. *Journal of the American Statistical Association* **90**: 773–795.

**Kephart S**, **Reynolds RJ**, **Rutter MT**, **Fenster CB**, **Dudash MR. 2006**. Pollination and seed predation by moths on *Silene* and allied Caryophyllaceae: evaluating a model system to study the evolution of mutualisms. *New Phytologist* **169**: 667–80.

**Kula AAR**, **Dudash MR**, **Fenster CB. 2013**. Choices and consequences of oviposition by a pollinating seed predator, *Hadena ectypa* (Noctuidae), on its host plant, *Silene stellata* (Caryophyllaceae). *American Journal of Botany* **100**: 1148–1154.

**Kula AAR**, **Castillo DM**, **Dudash MR**, **Fenster CB. 2014**. Interactions between a pollinating seed predator and its host plant: the role of environmental context within a population. *Ecology and Evolution* **4**: 2901–2912.

**Magalhaes IS**, **Gleiser G**, **Labouche A-M**, **Bernasconi G. 2011**. Comparative population genetic structure in a plant–pollinator/seed predator system. *Molecular Ecology* **20**: 4618–4630.

**Meirmans PG. 2012**. AMOVA-based clustering of population genetic data. *Journal of Heredity* **103**: 744–750.

**Meirmans PG. 2013**. *GenoDive (version 2.0 b23, manual): software for analysis of population genetic data*. Universiteit van Amsterdam.

**Meirmans PG**, **Van Tienderen PH. 2004**. GENOTYPE and GENODIVE: two programs for the analysis of genetic diversity of asexual organisms. *Molecular Ecology Notes* **4**: 792–794.

**Moody ME**, **Mueller LD**, **Soltis DE. 1993**. Genetic variation and random drift in autotetraploid populations. *Genetics* **134**: 649–657.

**Nei M. 1987**. *Molecular evolutionary genetics*. New York: Columbia University Press.

**Nelson MW. 2012**. Notes on a recently discovered population of *Hadena ectypa* (Morrison, 1875) (Noctuidae: Noctuinae: Hadenini) in Massachusetts. *Journal of the Lepidopterists' Society* **66**: 1–10.

**Nuismer SL**, **Thompson JN**, **Gomulkiewicz R. 1999**. Gene flow and geographically structured coevolution. *Proceedings of the Royal Society B: Biological Sciences* **266**: 605.

**Pettersson MW. 1991**. Pollination by a guild of fluctuating moth populations: option for unspecialization in *Silene vulgaris*. *Journal of Ecology* **79**: 591–604.

**Popp M**, **Oxelman B. 2007**. Origin and evolution of North American polyploid *Silene* (Caryophyllaceae). *American Journal of Botany* **94**: 33–349.

**Prieto-Benítez S**, **Dötterl S**, **Giménez-Benavides L. 2016**. Circadian rhythm of a *Silene* species favours nocturnal pollination and constrains diurnal visitation. *Annals of Botany* **118**: 907–918.

**Pritchard JK**, **Stephens M**, **Donnelly P. 2000**. Inference of population structure using multilocus genotype data. *Genetics* **155**: 945–959.

**Pritchard JK**, **Wen X**, **Falush D. 2010**. *Documentation for structure software: Version 2.3*. Chicago, IL: University of Chicago.

**Ramasamy RK**, **Ramasamy S**, **Bindroo BB**, **Naik VG. 2014**. STRUCTURE PLOT: a program for drawing elegant STRUCTURE bar plots in user friendly interface. *SpringerPlus* **3**: 431.

**Reed DH**, **Frankham R. 2001**. How closely correlated are molecular and quantitative measures of genetic variation? A meta-analysis. *Evolution* **55**: 1095–1103.

**Reynolds RJ. 2009**. Pollinator specialization and the evolution of pollination syndromes in the related *Silene*, *S. caroliniana*, *S. virginica*, and *S. stellata*. *Ecology* **90**: 2077–2087.

**Reynolds RJ**, **Kula AAR**, **Fenster CB**, **Dudash MR. 2012**. Variable nursery pollinator importance and its effect on plant reproductive success. *Oecologia* **168**: 439–448.

**Reynolds RJ**, **Westbrook MJ**, **Rohde AS**, **Cridland JM**, **Fenster CB**, **Dudash MR. 2009**. Pollinator specialization and pollination syndromes of three related North American *Silene*. *Ecology* **90**: 2077–2087.

**Rhodes MK**, **Fant JB**, **Skogen KA. 2014**. Local topography shapes fine-scale spatial genetic structure in the Arkansas Valley evening primrose, *Oenothera harringtonii* (Onagraceae). *Journal of Heredity* **105**: 900–909.

**Richards CM. 2000**. Inbreeding depression and genetic rescue in a plant metapopulation. *American Naturalist* **155**: 383–394.

**Richards CM**, **Emery SN**, **McCauley DE. 2003**. Genetic and demographic dynamics of small populations of *Silene latifolia*. *Heredity* **90**: 181–186.

**Schweitzer DF**, **Minno MC**, **Wagner DL. 2011**. *Rare, declining, and poorly known butterflies and moths (Lepidoptera) of forests and woodlands in the eastern United States*. Morgantown, WV: US Forest Service, Forest Health Technology Enterprise Team.

**Thompson JN. 2005**. *The geographic mosaic of coevolution*. Chicago, IL: University of Chicago Press.

**Tilman D**, **Kareiva PM. 1997**. *Spatial ecology: the role of space in population dynamics and interspecific interactions*. Princeton, NJ: Princeton University Press.

**Truong C**, **Palmé AE**, **Felber F. 2007**. Recent invasion of the mountain birch *Betula pubescens* ssp. *tortuosa* above the treeline due to climate change: genetic and ecological study in northern Sweden. *Journal of Evolutionary Biology* **20**: 369–380.

**Whelan RJ**, **Ayre DJ**, **Beynon FM. 2009**. The birds and the bees: pollinator behaviour and variation in the mating system of the rare shrub *Grevillea macleayana*. *Annals of Botany* **103**: 1395–1401.

**Zhou J. 2017**. *Natural selection, population genetics, and trait diversification of Silene stellata and its pollinating seed predator Hadena ectypa*. PhD thesis, University of Maryland.

**Zhou J**, **Dudash MR**, **Fenster CB. 2016*a***. Cannibalism during early larval development of *Hadena ectypa* Morrison (Lepidoptera: Noctuidae). *Proceedings of the Entomological Society of Washington* **118**: 450–455.

**Zhou J**, **Dudash MR**, **Fenster CB**, **Zimmer EA. 2016*b***. Development of highly variable microsatellite markers for the tetraploid *Silene stellata* (Caryophyllaceae). *Applications in Plant Sciences* **4**: apps.1600117. doi: 10.3732/apps.1600117.